

A framework for linear and nonlinear S-wave and C-wave time-lapse difference AVO

Shahin Jabbari and Kristopher A. Innanen

ABSTRACT

Multicomponent time-lapse amplitude variation with offset (AVO) may improve approximating time-lapse difference data. The difference data during the change in a reservoir from the baseline survey relative to the monitor survey are described for shear wave, and converted waves. We defined a framework for the difference reflection data, $\Delta R_{SS}(\theta)$, $\Delta R_{PS}(\theta)$, and $\Delta R_{SP}(\theta)$, in order of physical change or baseline interface contrast and time-lapse changes. A framework for linear and non linear time-lapse difference data are formulated using amplitude variation with offset (AVO) methods. The higher order terms represent corrections appropriate for large contrasts. We conclude that in many plausible time-lapse scenarios the increase in accuracy associated with higher order corrections is non-negligible for shear wave and converted wave as well as P-wave.

INTRODUCTION

Production or employment of enhanced oil recovery techniques (EOR) will affect the reservoir properties such as fluid flow and pressure. 4D Time-lapse extends the useful life of an oilfield by monitoring these changes. Prior to utilizing a reservoir, a first seismic experiment called the baseline survey is acquired, and after a particular interval of time following several geological/geophysical changes, another seismic survey, called a monitor survey, is acquired and then compared with the baseline survey (Greaves and Fulp, 1987; M. Landrø and Strønen, 1999; Lumley, 2001). The measurable difference in the seismic trace between the baseline and monitor survey, difference data, can be in amplitude, frequency, polarity, or the location of the interfaces. Perturbation (scattering) theory and amplitude variation with offset (AVO) methods can be used as a framework to model the difference data in a time lapse survey. The baseline survey is taken to describe the background medium against which to measure the perturbation detected in the monitor survey. The perturbation quantifies the changes in P wave and S wave velocities and density from the time of the baseline relative to the monitor survey (Innanen et al., 2013).

AVO methods indicate a nonlinear relationship between the pressure and saturation changes and P wave velocity change. Indeed, there is a highly non-linear relationship between P wave velocity change and the pressure change in a reservoir, demanding the use of higher order terms (Landrø, 2001).

A framework has been formulated to model linear and nonlinear elastic time-lapse difference AVO ($\Delta R_{PP}(\theta)$) for P-P sections (Jabbari and Innanen, 2013). The study described here focuses on applying the perturbation theory in a time-lapse amplitude variation with offset (Time-lapse AVO) method to model a framework to describe the difference data for the converted wave and shear wave.

Although P-wave seismic is the primary survey method in seismology, using multicom-

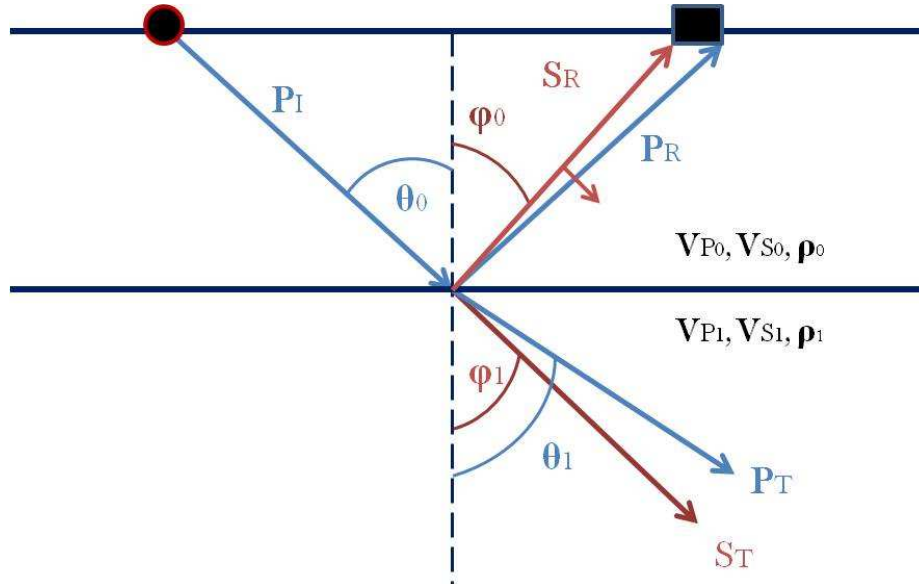


FIG. 1. Displacement amplitude of an incident P-wave with related reflected and transmitted P and S waves.

ponent recording can improve and support P-wave seismic data, specially for rocks with similar p-wave properties which may show a greater variation in S-wave properties (Figure 1). Multicomponent surveying has developed rapidly in both land and marine acquisition and processing techniques, with many applications in structural imaging, lithologic estimation, anisotropy analysis, and reservoir monitoring. The elastic properties of a rock, as well as acoustic properties, changes when the pressure and fluid flow is altered in a reservoir due to production. This raise the necessity of multicomponent 4D time-lapse analysis in a reservoir (Stewart et al., 2002, 2003).

Theory

We will consider two seismic experiments involved in a time-lapse survey, a baseline survey followed by a monitoring survey. The P-wave and S-wave velocities and the density change from the time of the baseline survey relative to the monitoring survey. This pair of models is consistent with an unchanging cap rock overlying a porous target which is being produced. Let V_{P_0}, V_{S_0}, ρ_0 and V_{P_b}, V_{S_b}, ρ_b be the rock properties of the cap rock and reservoir at the time of the baseline survey. Amplitudes of reflected and transmitted P and S waves impinging on the boundary of a planar interface between these two elastic media are calculated through setting the boundary conditions in the Zoeppritz equations which can be rearranged in matrix form e.g. (Aki and Richards, 2002):

$$P \begin{bmatrix} R_{PP} \\ R_{PS} \\ T_{PP} \\ T_{PS} \end{bmatrix} = b_P \quad \text{and} \quad S \begin{bmatrix} R_{SS} \\ R_{SP} \\ T_{SS} \\ T_{SP} \end{bmatrix} = b_S, \quad (1)$$

where

$$P \equiv \begin{bmatrix} -X & -\sqrt{1-B^2X^2} & CX & \sqrt{1-D^2X^2} \\ \sqrt{1-X^2} & -BX & \sqrt{1-C^2X^2} & -DX \\ 2B^2X\sqrt{1-X^2} & B(1-2B^2X^2) & 2AD^2X\sqrt{1-C^2X^2} & AD(1-2D^2X^2) \\ -1+2B^2X^2 & 2B^2X\sqrt{1-B^2X^2} & AC(1-2D^2X^2) & -2AD^2X\sqrt{1-D^2X^2} \end{bmatrix}, \quad (2)$$

$$S \equiv \begin{bmatrix} Y & -\sqrt{1-B'^2Y^2} & FY & -\sqrt{1-E^2Y^2} \\ -\sqrt{1-Y^2} & -B'Y & \sqrt{1-F^2Y^2} & EY \\ -2Y\sqrt{1-Y^2} & B'(1-2X^2) & 2AF^2Y\sqrt{1-F^2Y^2} & -AE(1-2F^2Y^2) \\ 1-2Y^2 & 2Y\sqrt{1-B'^2Y^2} & AF(1-2F^2Y^2) & 2AF^2Y\sqrt{1-E^2Y^2} \end{bmatrix}, \quad (3)$$

$X = \sin \theta$, θ is the P-wave incident angle, and $Y = \sin \phi$, ϕ is the S-wave incident angle, and

$$b_P \equiv \begin{bmatrix} X \\ \sqrt{1-X^2} \\ 2B^2X\sqrt{1-X^2} \\ 1-2B^2X^2 \end{bmatrix}, \quad \text{and} \quad b_S \equiv \begin{bmatrix} Y \\ \sqrt{1-Y^2} \\ 2Y\sqrt{1-Y^2} \\ 1-2Y^2 \end{bmatrix}, \quad (4)$$

The ratio of elastic parameters are defined as:

$$A \equiv \frac{\rho_1}{\rho_0}, \quad B \equiv \frac{V_{S_0}}{V_{P_0}}, \quad B' \equiv \frac{V_{P_0}}{V_{S_0}}, \quad C \equiv \frac{V_{P_1}}{V_{P_0}}, \quad D \equiv \frac{V_{S_1}}{V_{P_0}}, \quad E \equiv \frac{V_{P_1}}{V_{S_0}}, \quad F \equiv \frac{V_{S_1}}{V_{S_0}}. \quad (5)$$

Reflection coefficients are determined by using Cramer's rule and forming auxiliary matrices P_P and P_S by replacing the first and then second columns of P with b_P , and then forming a further two auxiliary matrices S_S and S_P by replacing the first and then second columns of S with b_S :

$$R_{PP}(\theta) = \frac{\det(P_P)}{\det(P)}, \quad R_{PS}(\theta) = \frac{\det(P_S)}{\det(P)}, \quad R_{SS}(\phi) = \frac{\det(S_S)}{\det(S)}, \quad R_{SP}(\phi) = \frac{\det(S_P)}{\det(S)}. \quad (6)$$

R_{PP} , R_{PS} , R_{SS} , and R_{SP} for the monitor survey are calculated using the same method. Rock properties for cap rock are the same, but reservoir properties change to V_{P_m} , V_{S_m} , ρ_m . The difference data reflection coefficients between the baseline and monitor survey is then calculated as:

$$\begin{aligned} \Delta R_{PP}(\theta) &= R_{PP}^m(\theta) - R_{PP}^b(\theta) \\ \Delta R_{PS}(\theta) &= R_{PS}^m(\theta) - R_{PS}^b(\theta) \\ \Delta R_{SS}(\phi) &= R_{SS}^m(\phi) - R_{SS}^b(\phi) \\ \Delta R_{SP}(\phi) &= R_{SP}^m(\phi) - R_{SP}^b(\phi). \end{aligned} \quad (7)$$

In our time lapse study we have considered two groups of perturbation parameters (Innanen et al., 2013; Stolt and Weglein, 2012). we use the same standard scattering nomenclature found in e.g. Stolt and Weglein (2012). The first group expresses the perturbation caused by propagating the wavefield from the first medium to the second medium in the baseline survey:

$$b_{VP} = 1 - \frac{V_{P_0}^2}{V_{P_b}^2}, \quad b_{VS} = 1 - \frac{V_{S_0}^2}{V_{S_b}^2}, \quad b_\rho = 1 - \frac{\rho_0}{\rho_b}. \quad (8)$$

The second group is to account for the change from the baseline survey relative to the monitor survey, the time lapse perturbation, we define:

$$a_{VP} = 1 - \frac{V_{P_b}^2}{V_{P_m}^2}, \quad a_{VS} = 1 - \frac{V_{S_b}^2}{V_{S_m}^2}, \quad a_\rho = 1 - \frac{\rho_b}{\rho_m}. \quad (9)$$

Elastic parameters may re-defined in terms of perturbations in P-wave and S-wave velocities and the densities as:

$$\begin{aligned} A &= (1 - b_\rho)^{-1} \times (1 - a_\rho)^{-1}, \\ C &= (1 - b_{VP})^{-\frac{1}{2}} \times (1 - a_{VP})^{-\frac{1}{2}}, \\ D &= \frac{V_{S_0}}{V_{P_0}} \times (1 - b_{VS})^{-\frac{1}{2}} \times (1 - a_{VS})^{-\frac{1}{2}}, \\ E &= \frac{V_{P_0}}{V_{S_0}} \times (1 - b_{VP})^{-\frac{1}{2}} \times (1 - a_{VP})^{-\frac{1}{2}}, \\ F &= (1 - b_{VS})^{-\frac{1}{2}} \times (1 - a_{VS})^{-\frac{1}{2}} \end{aligned} \quad (10)$$

These forms are substituted into equation (2) and (3), and the determinants and determinations in equation (6) are expanded in orders of all six perturbations, $\sin^2 \theta$, and $\sin^2 \phi$.

$$\begin{aligned} \Delta R_{PP}(\theta) &= \Delta R_{PP}^{(1)}(\theta) + \Delta R_{PP}^{(2)}(\theta) + \Delta R_{PP}^{(3)}(\theta) + \dots \\ \Delta R_{PS}(\theta) &= \Delta R_{PS}^{(1)}(\theta) + \Delta R_{PS}^{(2)}(\theta) + \Delta R_{PS}^{(3)}(\theta) + \dots \\ \Delta R_{SS}(\phi) &= \Delta R_{SS}^{(1)}(\phi) + \Delta R_{SS}^{(2)}(\phi) + \Delta R_{SS}^{(3)}(\phi) + \dots \\ \Delta R_{SP}(\phi) &= \Delta R_{SP}^{(1)}(\phi) + \Delta R_{SP}^{(2)}(\phi) + \Delta R_{SP}^{(3)}(\phi) + \dots \end{aligned} \quad (11)$$

$\Delta R_{PP}(\theta)$ for first order, second order, and third order can be found in Jabbari and Innanen (2013). Reflection coefficient difference data for converted wave and shear wave are presented in the following section.

Time-lapse difference data for converted wave and shear wave

Linear and higher order terms for a down going p-wave and upcoming S-wave are:

$$\begin{aligned}
 \Delta R_{PS}^{(1)}(\theta) &= \left[-\frac{V_{S_0}}{V_{P_0}} \sin \theta \right] a_{VS} + \left[-\frac{1}{2} \left(2\frac{V_{S_0}}{V_{P_0}} + 1 \right) \sin \theta \right] a_{\rho} \\
 \Delta R_{PS}^{(2)}(\theta) &= \left[-\frac{3}{4} \frac{V_{S_0}}{V_{P_0}} \sin \theta \right] a_{VS}^2 + \left[-\frac{1}{2} \sin \theta \right] a_{\rho}^2 + \left[\frac{1}{2} \left(2\frac{V_{S_0}}{V_{P_0}} - 1 \right) \sin \theta \right] b_{\rho} a_{\rho} \\
 &\quad + \left[-\frac{1}{2} \frac{V_{S_0}}{V_{P_0}} \sin \theta \right] b_{VS} a_{VS} + \left[\frac{1}{4} \frac{V_{S_0}}{V_{P_0}} \sin \theta \right] (a_{VP} a_{VS} + a_{VP} b_{VS} + b_{VP} a_{VS}) \\
 &\quad + \left[\frac{1}{8} \left(2\frac{V_{S_0}}{V_{P_0}} - 1 \right) \sin \theta \right] (a_{VP} a_{\rho} + b_{\rho} a_{VP} + a_{\rho} b_{VP} + a_{\rho} a_{VS} + a_{\rho} b_{VS} + b_{\rho} a_{VS}) \\
 \Delta R_{PS}^{(3)}(\theta) &= \left[-\frac{5}{8} \frac{V_{S_0}}{V_{P_0}} \sin \theta \right] a_{VS}^3 + \left[\frac{1}{8} \left(2\frac{V_{S_0}}{V_{P_0}} - 3 \right) \sin \theta \right] a_{\rho}^3 + \left[-\frac{3}{8} \frac{V_{S_0}}{V_{P_0}} \sin \theta \right] \\
 &\quad (b_{VS} a_{VS}^2 + b_{VS}^2 a_{VS}) + \left[\frac{1}{16} \left(6\frac{V_{S_0}}{V_{P_0}} - 1 \right) \sin \theta \right] (a_{\rho}^2 a_{VS} + b_{\rho}^2 a_{VS} + a_{\rho}^2 b_{VS}) + \\
 &\quad \left[\frac{1}{16} \left(4\frac{V_{S_0}}{V_{P_0}} - 1 \right) \sin \theta \right] (a_{\rho} b_{VS}^2 + a_{\rho} a_{VS}^2 + b_{\rho} a_{VS}^2) + \left[\frac{1}{16} \left(2\frac{V_{S_0}}{V_{P_0}} - 1 \right) \right. \\
 &\quad \left. \sin \theta \right] (b_{\rho} a_{VP}^2 + b_{\rho}^2 a_{VP} + a_{\rho} b_{VP}^2 + a_{\rho}^2 b_{VP} + a_{\rho}^2 a_{VP} + a_{\rho} a_{VP}^2) + \\
 &\quad \left[\frac{1}{8} \frac{V_{S_0}}{V_{P_0}} \sin \theta \right] (b_{VP}^2 a_{VS} + a_{VP}^2 b_{VS} + a_{VP}^2 a_{VS} + b_{VP} b_{VS} a_{VS} + a_{VP} b_{VS} a_{VS}) \\
 &\quad + \left[\frac{1}{8} \left(6\frac{V_{S_0}}{V_{P_0}} - 1 \right) \sin \theta \right] (b_{\rho}^2 a_{\rho} + b_{\rho} a_{\rho}^2) + \left[\frac{1}{32} \left(2\frac{V_{S_0}}{V_{P_0}} - 1 \right) \sin \theta \right] (a_{\rho} b_{VP} a_{VS} \\
 &\quad + a_{\rho} b_{VP} b_{VS} + b_{\rho} a_{VP} a_{VS} + b_{\rho} a_{VP} b_{VS} + a_{\rho} a_{VP} a_{VS} + a_{\rho} a_{VP} b_{VS} + b_{\rho} b_{VP} a_{VS}) \\
 &\quad \left[\frac{1}{4} \frac{V_{S_0}}{V_{P_0}} \sin \theta \right] (b_{\rho} b_{VS} a_{VS} + a_{\rho} b_{VS} a_{VS}) + \left[\frac{1}{2} \frac{V_{S_0}}{V_{P_0}} \sin \theta \right] (b_{\rho} a_{\rho} a_{VS} + b_{\rho} a_{\rho} b_{VS}) \\
 &\quad + \left[\frac{3}{16} \frac{V_{S_0}}{V_{P_0}} \sin \theta \right] (a_{VP} b_{VS}^2 + a_{VP} a_{VS}^2 + b_{VP} a_{VS}^2)
 \end{aligned} \tag{12}$$

Firs, second, and third order terms for time-lapse difference data for a down going S-wave and upcoming P-wave are:

$$\begin{aligned}
 \Delta R_{SP}^{(1)}(\phi) &= \left[-\frac{V_{S_0}}{V_{P_0}} \sin \phi \right] a_{VS} + \left[-\frac{1}{2} \left(2\frac{V_{S_0}}{V_{P_0}} + 1 \right) \sin \phi \right] a_\rho \\
 \Delta R_{SP}^{(2)}(\phi) &= \left[-\left(\frac{3}{4} \right) \frac{V_{S_0}}{V_{P_0}} \sin \phi \right] a_{VS}^2 + \left[-\frac{1}{2} \sin \phi \right] a_\rho^2 + \left[\frac{1}{2} \left(2\frac{V_{S_0}}{V_{P_0}} - 1 \right) \sin \phi \right] b_\rho a_\rho \\
 &\quad + \left[-\left(\frac{1}{2} \right) \frac{V_{S_0}}{V_{P_0}} \sin \phi \right] b_{VS} a_{VS} + \left[\left(\frac{1}{4} \right) \frac{V_{S_0}}{V_{P_0}} \sin \phi \right] (a_{VP} a_{VS} + a_{VP} b_{VS} + b_{VP} a_{VS}) \\
 &\quad + \left[\frac{1}{8} \left(2\frac{V_{S_0}}{V_{P_0}} - 1 \right) \sin \phi \right] (a_{VP} a_\rho + b_\rho a_{VP} + a_\rho b_{VP} + a_\rho a_{VS} + a_\rho b_{VS} + b_\rho a_{VS}) \\
 \Delta R_{SP}^{(3)}(\phi) &= \left[\left(\frac{3}{8} \right) \frac{V_{S_0}}{V_{P_0}} \sin \phi \right] a_{VS}^3 + \left[\frac{1}{8} \left(10\frac{V_{S_0}}{V_{P_0}} + 1 \right) \sin \phi \right] (a_\rho^3 + b_{VS} b_\rho a_{VS} + b_{VS} a_\rho a_{VS} \\
 &\quad + b_\rho a_{VS}^2 + a_\rho a_{VS}^2 + a_\rho b_{VS}^2) + \left[\frac{1}{32} \left(2\frac{V_{S_0}}{V_{P_0}} - 1 \right) \sin \phi \right] (b_{VP} b_\rho a_{VS} + \\
 &\quad b_{VP} a_\rho a_{VS} + b_{VS} b_\rho a_{VP} + b_{VS} a_\rho a_{VP} + b_{VP} a_\rho b_{VS} + a_{VP} b_\rho a_{VS} + a_{VP} a_\rho a_{VS}) \\
 &\quad + \left[\frac{1}{4} \left(6\frac{V_{S_0}}{V_{P_0}} + 1 \right) \sin \phi \right] (a_\rho b_\rho a_{VS} + a_\rho b_\rho b_{VS}) + \left[\frac{1}{16} \left(22\frac{V_{S_0}}{V_{P_0}} + 3 \right) \sin \phi \right] \\
 &\quad (a_{VS} a_\rho^2 + b_{VS} a_\rho^2 + a_{VS} b_\rho^2) + \left[\frac{1}{8} \left(14\frac{V_{S_0}}{V_{P_0}} + 3 \right) \sin \phi \right] (b_\rho a_\rho^2 + a_\rho b_\rho^2) \left[\frac{1}{16} + \right. \\
 &\quad \left. \left(2\frac{V_{S_0}}{V_{P_0}} - 1 \right) \sin \phi \right] (b_{VP} a_\rho^2 + a_{VP} b_\rho^2 + a_{VP} a_\rho^2 + a_{VP}^2 b_\rho + a_{VP}^2 a_\rho + b_{VP}^2 a_\rho) \\
 &\quad + \left[\left(\frac{5}{8} \right) \frac{V_{S_0}}{V_{P_0}} \sin \phi \right] (a_{VS} b_{VS}^2 + b_{VS} a_{VS}^2) + \left[\left(\frac{1}{8} \right) \frac{V_{S_0}}{V_{P_0}} \sin \phi \right] (a_{VS} b_{VP}^2 + b_{VS} a_{VP}^2 + a_{VS} a_{VP}^2 \\
 &\quad + a_{VS} b_{VS} a_{VP} + a_{VS} b_{VS} b_{VP}) + \left[\left(\frac{3}{16} \right) \frac{V_{S_0}}{V_{P_0}} \sin \phi \right] (b_{VP} a_{VS}^2 + a_{VP} b_{VS}^2 + a_{VP} a_{VS}^2)
 \end{aligned} \tag{13}$$

The results for shear wave, down going S-wave and upcoming S-wave are:

$$\begin{aligned}
 \Delta R_{SS}^{(1)}(\phi) &= \left[\frac{1}{4} (7 \sin^2 \phi - 1) \right] a_{VS} + \left[\frac{1}{2} (4 \sin^2 \phi - 1) \right] a_{\rho} \\
 \Delta R_{SS}^{(2)}(\phi) &= \left[\left(\frac{7}{4} - \frac{V_{S_0}}{V_{P_0}} \right) \sin^2 \phi - \frac{1}{8} \right] a_{VS}^2 + \left[\left(1 + \left(\frac{1}{4} \right) \frac{V_{P_0}}{V_{S_0}} - \frac{V_{S_0}}{V_{P_0}} \right) \sin^2 \phi - \frac{1}{4} \right] a_{\rho}^2 \\
 &\quad + \left[\left(1 - 2 \frac{V_{S_0}}{V_{P_0}} \right) \sin^2 \phi \right] (a_{VS} a_{\rho} + a_{VS} b_{\rho} + b_{VS} a_{\rho}) \\
 &\quad + \left[\left(\frac{7}{4} - 2 \frac{V_{S_0}}{V_{P_0}} \right) \sin^2 \phi \right] (a_{VS} b_{VS}) + \left[\left(\left(\frac{1}{2} \right) \frac{V_{P_0}}{V_{S_0}} - 2 \frac{V_{S_0}}{V_{P_0}} \right) \sin^2 \phi \right] (a_{\rho} b_{\rho}) \\
 \Delta R_{SS}^{(3)}(\phi) &= \frac{1}{64} \left[5 - \left(96 \frac{V_{S_0}}{V_{P_0}} + 63 \right) \sin^2 \phi \right] a_{VS}^3 + \frac{1}{8} \left[\left(3 \frac{V_{P_0}}{V_{S_0}} - 4 \frac{V_{S_0}}{V_{P_0}} - 16 \right) \right. \\
 &\quad \left. \sin^2 \phi + 3 \right] a_{\rho}^3 + \frac{1}{4} \sin^2 \phi (a_{VP} a_{VS}^2 + a_{VP} b_{VS}^2 + b_{VP} a_{VS}^2) \\
 &\quad + \frac{1}{32} \left[7 - \left(48 \frac{V_{S_0}}{V_{P_0}} + 78 \right) \sin^2 \phi \right] (b_{\rho} a_{VS}^2 + a_{\rho} a_{VS}^2 + a_{\rho} b_{VS}^2) \\
 &\quad + \frac{1}{64} \left[7 - \left(160 \frac{V_{S_0}}{V_{P_0}} + 125 \right) \sin^2 \phi \right] (b_{VS} a_{VS}^2 + a_{VS} b_{VS}^2) \\
 &\quad + \frac{1}{8} \left[\left(2 \frac{V_{P_0}}{V_{S_0}} + 8 \frac{V_{S_0}}{V_{P_0}} - 35 \right) \sin^2 \phi + 3 \right] (b_{VS} b_{\rho} a_{\rho} + a_{VS} b_{\rho} a_{\rho}) \\
 &\quad + \frac{1}{4} \left[\left(2 \frac{V_{S_0}}{V_{P_0}} - 1 \right) \sin^2 \phi \right] (b_{VS} b_{VP} a_{\rho} + b_{VS} a_{VP} b_{\rho} + a_{VP} a_{VS} a_{\rho} + a_{VS} a_{VP} b_{\rho} \\
 &\quad + a_{VS} b_{VP} a_{\rho} + b_{VP} a_{VS} b_{\rho} + b_{VS} a_{VP} a_{\rho}) + \frac{1}{8} \left[\left(\frac{V_{P_0}}{V_{S_0}} + 4 \frac{V_{S_0}}{V_{P_0}} \right. \right. \\
 &\quad \left. \left. - 4 \right) \sin^2 \phi \right] (b_{VP} a_{\rho} b_{\rho} + a_{VP} a_{\rho} b_{\rho}) + \frac{1}{16} \left[\left(\frac{V_{P_0}}{V_{S_0}} + 4 \frac{V_{S_0}}{V_{P_0}} - 4 \right) \sin^2 \phi \right] \\
 &\quad (a_{VP} b_{\rho}^2 + a_{VP} a_{\rho}^2 + b_{VP} a_{\rho}^2) + \frac{1}{2} \left[\frac{V_{S_0}}{V_{P_0}} \sin^2 \phi \right] (b_{VS} a_{VP} a_{VS} + b_{VP} b_{VS} a_{VS}) \\
 &\quad + \frac{1}{8} \left[\left(5 \frac{V_{P_0}}{V_{S_0}} + 4 \frac{V_{S_0}}{V_{P_0}} - 32 \right) \sin^2 \phi + 5 \right] (a_{\rho} b_{\rho}^2 + b_{\rho} a_{\rho}^2) \\
 &\quad + \frac{1}{16} \left[3 - \left(16 \frac{V_{S_0}}{V_{P_0}} + 54 \right) \sin^2 \phi \right] (b_{VS} a_{VS} a_{\rho} + b_{VS} a_{VS} b_{\rho}) \\
 &\quad + \frac{1}{16} \left[\left(2 \frac{V_{P_0}}{V_{S_0}} - 8 \frac{V_{S_0}}{V_{P_0}} - 47 \right) \sin^2 \phi + 5 \right] (a_{VS} b_{\rho}^2 + a_{VS} a_{\rho}^2 + b_{VS} a_{\rho}^2)
 \end{aligned} \tag{14}$$

Time-lapse AVO in terms of relative seismic parameter changes

The linear and higher order approximation solutions for ΔR are presented as expansions of the perturbation parameters in the previous section. We will compute time-lapse difference data in terms of relative changes in seismic parameters, $\frac{\Delta V_P}{V_P}$, $\frac{\Delta V_S}{V_S}$, and $\frac{\Delta \rho}{\rho}$, because this choice permits quantitative comparison with other studies in the literature, and

furthermore because AVO modelling series in order of relative change may have improved convergence properties (Innanen, 2013). We designate the capital delta symbol to indicate the relative changes in seismic parameters for the physical contrast between the cap rock and reservoir in the baseline survey. To present changes in the seismic parameters due to time lapse variations in the reservoir, we use a small delta symbol. The relative changes in the baseline survey are defined as follows:

$$\begin{aligned}\frac{\Delta V_P}{V_P} &= 2 \times \frac{V_{Pb} - V_{P0}}{V_{Pb} + V_{P0}}, \\ \frac{\Delta V_S}{V_S} &= 2 \times \frac{V_{Sb} - V_{S0}}{V_{Sb} + V_{S0}}, \\ \frac{\Delta \rho}{\rho} &= 2 \times \frac{\rho_b - \rho_0}{\rho_b + \rho_0},\end{aligned}\tag{15}$$

while time-lapse perturbations are defined as :

$$\begin{aligned}\frac{\delta V_P}{V_P} &= 2 \times \frac{V_{Pm} - V_{Pb}}{V_{Pm} + V_{Pb}}, \\ \frac{\delta V_S}{V_S} &= 2 \times \frac{V_{Sm} - V_{Sb}}{V_{Sm} + V_{Sb}}, \\ \frac{\delta \rho}{\rho} &= 2 \times \frac{\rho_m - \rho_b}{\rho_m + \rho_b}.\end{aligned}\tag{16}$$

To express our linear and higher order time lapse difference data results in terms of relative changes, we expand b_{VP} , b_{VS} , and ... in terms of the appropriate series of relative changes as:

$$\begin{aligned}b_{VP} &= 2 \left(\frac{\Delta V_P}{V_P} \right) - 2 \left(\frac{\Delta V_P}{V_P} \right)^2 + \frac{3}{2} \left(\frac{\Delta V_P}{V_P} \right)^3 - \dots \\ b_{VS} &= 2 \left(\frac{\Delta V_S}{V_S} \right) - 2 \left(\frac{\Delta V_S}{V_S} \right)^2 + \frac{3}{2} \left(\frac{\Delta V_S}{V_S} \right)^3 - \dots \\ b_\rho &= \left(\frac{\Delta \rho}{\rho} \right) - \frac{1}{2} \left(\frac{\Delta \rho}{\rho} \right)^2 + \frac{1}{4} \left(\frac{\Delta \rho}{\rho} \right)^3 + \dots,\end{aligned}\tag{17}$$

and

$$\begin{aligned}a_{VP} &= 2 \left(\frac{\delta V_P}{V_P} \right) - 2 \left(\frac{\delta V_P}{V_P} \right)^2 + \frac{3}{2} \left(\frac{\delta V_P}{V_P} \right)^3 - \dots \\ a_{VS} &= 2 \left(\frac{\delta V_S}{V_S} \right) - 2 \left(\frac{\delta V_S}{V_S} \right)^2 + \frac{3}{2} \left(\frac{\delta V_S}{V_S} \right)^3 - \dots \\ a_\rho &= \frac{\delta \rho}{\rho} - \frac{1}{2} \frac{\delta \rho^2}{\rho} + \frac{1}{4} \frac{\delta \rho^3}{\rho} + \dots,\end{aligned}\tag{18}$$

Substituting equation (17) and equation (18) into the equations for ΔR_{PP} , ΔR_{PS} , ΔR_{SP} , ΔR_{SS} and linearizing them, and assuming small angles such that $\sin^2 \theta \ll 1$ and $\sin^2 \phi \ll 1$

1,

$$\begin{aligned}
\Delta R_{PP}(\theta) &\sim \Delta R_{PP}^{(1)}(\theta) = \frac{1}{2} \left(\frac{\delta\rho}{\rho} + \frac{\delta V_P}{V_P} \right) - \sin^2 \theta \frac{2V_S^2}{V_P^2} \left(\frac{\delta\rho}{\rho} + 2\frac{\delta V_S}{V_S} \right) + \frac{\delta V_P}{2V_P} \sin^2 \theta \\
\Delta R_{SS}(\phi) &\sim \Delta R_{SS}^{(1)}(\phi) = \frac{1}{2} (7 \sin^2 \phi - 1) \frac{\delta V_S}{V_S} + \frac{1}{2} (4 \sin^2 \phi - 1) \frac{\delta\rho}{\rho} \\
\Delta R_{PS}(\theta) &\sim \Delta R_{PS}^{(1)}(\theta) = \left(-2\frac{V_S}{V_P} \sin \theta \right) \frac{\delta V_S}{V_S} - \frac{1}{2} \left(2\frac{V_S}{V_P} + 1 \right) \sin \theta \frac{\delta\rho}{\rho} \\
\Delta R_{SP}(\phi) &\sim \Delta R_{SP}^{(1)}(\phi) = \left(-2\frac{V_S}{V_P} \sin \phi \right) \frac{\delta V_S}{V_S} - \frac{1}{2} \left(2\frac{V_S}{V_P} + 1 \right) \sin \phi \frac{\delta\rho}{\rho}
\end{aligned} \tag{19}$$

Linearizing ΔR_{PP} , we recover Landrø's equation for approximation of the difference reflection data for P-P sections. The second and third order terms of the difference reflection data in terms of relative parameters can be derived using the same process.

Numerical example

In this section, we examine the derived linear and non linear difference time lapse AVO terms qualitatively with a numerical example. The exact difference data are compared with our derived linear and higher order approximations for down going P-wave and upcoming S-wave, and down going S-wave and upcoming P-wave in Figure 2. The second and third approximations are in better agreement with the exact difference data, especially for angles below the critical angle, which correspond to the range of study in this project.

CONCLUSION

Time-lapse measurements provide a tool to monitor the dynamic changes in subsurface properties during the time of the exploitation of a reservoir. Changes in the fluid saturation and pressure will have an impact in elastic parameters of subsurface, such as P wave and S wave velocities and density, which can be approximated by applying time-lapse AVO analysis methods. A well-developed AVO regimes analyses converted wave and shear waves AVO as well the P-wave AVO. Jabbari and Innanen have already investigated P-wave time-lapse AVO and showed that adding the higher order terms in ΔR_{PP} to the linear approximation for difference time-lapse data increases the accuracy of the ΔR_{PP} and corrects the error due to linearizing ΔR_{PP} (Jabbari and Innanen, 2013). In the current research, we extended this work by formulating a framework for the difference reflection data in ΔR_{SS} , ΔR_{PS} , and ΔR_{SP} . The results showed that, including higher order terms in ΔR for shear waves and converted wave improves the accuracy of approximating time lapse difference reflection data, particularly for large contrast cases. Comparing linear, second, and third order terms for ΔR_{PS} and ΔR_{SP} indicates as we are moving toward higher order approximations; ΔR_{PS} and ΔR_{SP} are different. This confirms the difference between exact ΔR_{PS} and ΔR_{SP} which does not show up in the linear approximation case.

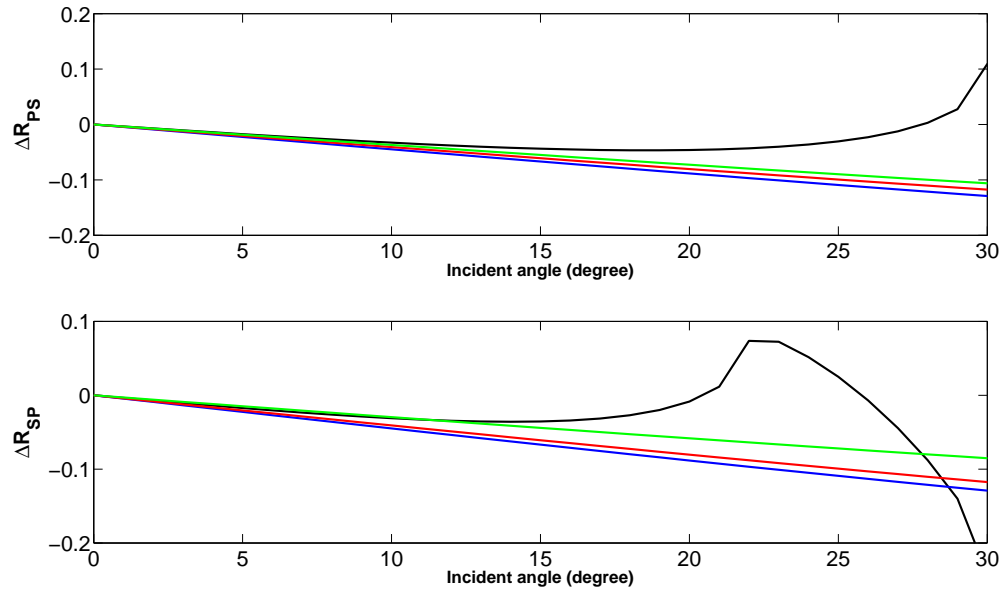


FIG. 2. ΔR_{PS} , and ΔR_{SP} for the exact, linear, second order, and third order approximation. Elastic incidence parameters: $V_{P0} = 2000\text{m/s}$, $V_{S0} = 1500\text{m/s}$ and $\rho_0 = 2.0\text{g/cc}$; Baseline parameters: $V_{PBL} = 3000\text{m/s}$, $V_{SBL} = 1700\text{m/s}$ and $\rho_{BL} = 2.1\text{g/cc}$; Monitor parameters: $V_{PBL} = 4000\text{m/s}$, $V_{SBL} = 1900\text{m/s}$ and $\rho_{BL} = 2.3\text{g/cc}$. Black: Exact difference data, Blue: Linear approximation, Red: Second order approximation, and Green: Third order approximation.

ACKNOWLEDGMENTS

We wish to thank sponsors, faculty, and staff of the Consortium for Research in Elastic Wave Exploration Seismology (CREWES) for their support of this work.

REFERENCES

- Aki, K., and Richards, P. G., 2002, Quantitative Seismology: University Science Books, 2 edn.
- Greaves, R. J., and Fulp, T., 1987, Three-dimensional seismic monitoring of an enhanced oil recovery process: *Geophysics*, **52**, 1175–1187.
- Innanen, K. A., 2013, Coupling in amplitude variation with offset and the wiggins approximation: *Geophysics*, **78**, No. 4, N21–N33.
- Innanen, K. A., Naghizadeh, M., and Kaplan, S. T., 2013, Perturbation methods for two special cases of the time-lapse seismic inverse problem: *Geophysical Prospecting*, accepted for publication.
- Jabbari, S., and Innanen, K. A., 2013, A framework for approximation of elastic time-lapse difference AVO signatures and validation on physical modeling data: 75th EAGE Conference and Exhibition incorporating SPE EUROPEC.
- Landrø, M., 2001, Discrimination between pressure and fluid saturation changes from time-lapse seismic data: *GEOPHYSICS*, **66**, No. 3, 836–844.
- Lumley, D., 2001, Time-lapse seismic reservoir monitoring: *Geophysics*, **66**, No. 1, 50–53.
- M. Landrø, E. H. B. E., O.A. Solheim, and Strønen, L. K., 1999, The gullfaks 4d seismic study: *Petr. Geosci.*, **5**, 213–226.

Stewart, R. R., Gaiser, J., Brown, R. J., and Lawton, D. C., 2002, Tutorial: converted-wave seismic exploration: methods: *Geophysics*, **67**, No. 5, 1348–1363.

Stewart, R. R., Gaiser, J., Brown, R. J., and Lawton, D. C., 2003, Tutorial: converted-wave seismic exploration: Application: *Geophysics*, **68**, No. 1, 40–57.

Stolt, R. H., and Weglein, A. B., 2012, *Seismic Imaging and Inversion: Volume 1: Application of Linear Inverse Theory*: Cambridge University Press.